Progress in Natural Science: Materials International 26 (2016) 232–236

HOSTED BY

Contents lists available at ScienceDirect

Progress in Natural Science: Materials International

journal homepage: www.elsevier.com/locate/pnsmi

Original Research

Flexible supercapacitor electrodes with vertically aligned carbon nanotubes grown on aluminum foils

Itir Bakis Dogru [a], Mete Batuhan Durukan [b], Onur Turel [b], Husnu Emrah Unalan [a,b,*]

[a] Micro and Nanotechnology Department, METU, Ankara 06800, Turkey
[b] Department of Metallurgical and Materials Engineering, METU, Ankara 06800 Turkey

ARTICLE INFO

Article history:
Received 30 March 2016
Accepted 20 April 2016
Available online 2 June 2016

Keywords:
Supercapacitor electrodes
Carbon nanotubes
Flexibility

ABSTRACT

In this work, vertically aligned carbon nanotubes (VACNTs) grown on aluminum foils were used as flexible supercapacitor electrodes. Aluminum foils were used as readily available, cheap and conductive substrates, and VACNTs were grown directly on these foils through chemical vapor deposition (CVD) method. Solution based ultrasonic spray pyrolysis (USP) method was used for the deposition of the CNT catalyst. Direct growth of VACNTs on aluminum foils ruled out both the internal resistance of the supercapacitor electrodes and the charge transfer resistance between the electrode and electrolyte. A specific capacitance of 2.61 mF/cm^2 at a scan rate of 800 mV/s was obtained from the fabricated electrodes, which is further improved through the bending cycles.

1. Introduction

As the electronic products develop into a more sophisticated form, the energy storage devices are also progressed to contain more capacity and functionality. In today's world, one of the most promising storage devices are supercapacitors; where the nanotechnology is directly applied within the electrodes [1]. There are numerous carbonaceous materials that are readily used and can potentially be used as supercapacitor electrodes, such as CNTs, carbon fibers, graphene and carbon aerogels [2–6]. All of which have different effects on the overall capacitance [7]. The nanoscale tubular morphology of CNTs offers low electrical resistivity [8]. Electrons can move along only in one direction, which is along the length of CNTs, forming a one dimensional material [9].

CVD growth of CNTs is very suitable for various applications since one can grow CNTs directly on a number of substrates [10]. There are numerous examples of the use of CNTs that are grown directly on conductive substrates or the use of CNTs with conductive additives in a composite form [11–16]. Synthesis of CNTs over large areas [17–19] is also possible, which makes CVD method unique and cost-effective. This method also enables the synthesis of patterned CNTs on predefined regions [20]. CNT growth by CVD method proceeds by two steps, namely catalyst preparation and CNT growth. The former affects the reconstruction of the catalyst thin film into islands, while the latter initiates CNT growth around these islands. Both steps dictate the morphology of the CNTs [21].

Flexible supercapacitors are suitable for many applications like roll-up displays and wearable electronics [22,23]. CNT based electrodes are commonly used for flexible supercapacitors [24,25]. In supercapacitor applications, entangled CNTs offer slow ion and electron movement due to their complex structure that prevents the ion diffusion to each CNT. Conversely, VACNT based electrodes offer higher performance since they have more surface area compared to entangled CNTs, which is available for the diffusion of electrolytes. The homogeneous distribution of CNTs and well-ordered alignment increases the density of CNTs as well as their supercapacitor performance [7,26,27].

It is valuable to grow VACNT forests on flexible substrates. Herein we present VACNT forests grown on aluminum foils as flexible supercapacitor electrodes. In terms of low density and high conductivity; aluminum is the third most abundant element in the world [28]. Moreover, we used USP method for the deposition of the catalyst. While most of the catalyst deposition methods operate under vacuum and require specified equipment for vacuum delivery, catalyst deposition by USP technique not only provides low cost and express deposition but also a homogeneous catalyst distribution over large areas. Since aluminum has a naturally oxidized surface, catalyst deposition without a support layer can be directed with less effort [29]. Although the melting point of aluminum is not as high as most of the other substrate types, direct growth of CNTs on aluminum foils can be achieved through controlled CVD parameters. When utilized as supercapacitor electrodes, VACNTs on aluminum foils show good cyclic stability and low resistance that make them ideal electrodes for energy storage devices [30].

* Corresponding author.
E-mail address: unalan@metu.edu.tr (H.E. Unalan).
Peer review under responsibility of Chinese Materials Research Society.

http://dx.doi.org/10.1016/j.pnsc.2016.05.011

2. Experimental

Aluminum foils are soft, flexible, ductile and cheap. They also possess good electrical conductivity. Pure aluminum foils were used in this work (Alfa Aesar, 0.025 mm thick, 99.45% metal basis). Foils were first cleaned with acetone (99.8%), isopropanol (99.8%) and distilled water (18.3 MΩ) sequentially, through simple immersion into these solvents for 10 min each. Soon after, foils were dried in a furnace at 80 °C. Following this cleaning, aluminum foils were deposited with catalyst to be able to grow CNTs through CVD method.

To deposit iron catalyst onto aluminum foils, a 5×10^{-3} M ethanolic solution containing iron (III) chloride hexahydrate (Sigma Aldrich, $FeCl_3 . 6H_2O$, 97%) was prepared and deposited via USP method [31]. Aluminum foils (8 cm × 6 cm) were placed on a heater set to 155 °C and deposited with catalyst. 5 ml ultrasonicated solution was sprayed from a distance of 5.25 cm with a 60 ml/h feeding rate. Heater was mounted on an x-y stage to allow homogeneous deposition of the catalyst onto the foils. Since aluminum has a native oxide layer, it was not necessary to deposit a support layer in case of USP. It was noticed that this native oxide layer prevents the diffusion of the catalyst towards the substrate, making this method quite practical. Following the USP deposition of the catalyst, foils were annealed in a furnace under air ambient at 500 °C for 1 h for the oxidation of iron catalyst.

Following the catalyst deposition, the foils were loaded to the CVD system. An Aixtron – Nano-instruments Black Magic II plasma enhanced PECVD system was used for the CNT synthesis. The system was fully computer controlled, which allowed precise control over the growth parameters improving the reproducibility of the growth results. Within the system, it was possible and very simple to alter the growth parameters like temperature, gas flow rates and pressure at any moment.

For CNT growth, the chamber was first vacuumed down to 0.1 mbar and then the pressure was set to 8 mbar and kept constant during the entire process. 200 sccm hydrogen (H_2) was introduced to the system and temperature was then increased to 600 °C at a rate of 200 °C/min. Samples were annealed at this temperature for 2 min. At the end of the annealing process, the precursor gas, acetylene (C_2H_2) was introduced into the system at a flow rate of 20 sccm, which initiated the CNT growth. At this stage, temperature was raised to 620 °C with a heating rate of 25 °C/min. At this temperature, the growth lasted for 5 min. At the end of the growth H_2 and C_2H_2 flows were stopped and the chamber was cooled by means of nitrogen (N_2) flow (1000 sccm). The samples were collected following venting.

The morphology of the fabricated CNTs was investigated by scanning electron microscopy (SEM, FEI Nova Nano SEM 430, operated at 10 kV). The samples were analyzed as is without the need for extra gold coating. Transmission electron microscopy (TEM) was performed on a JEOL TEM 2100 F microscope, operated at 200 kV. TEM samples were simply prepared from the ethanolic solution of samples scraped off the foils. Raman spectroscopy was used as a fast and nondestructive characterization method for CNTs. A Horiba Jobin Yvon iHR550 (532 nm wavelength) Raman system was used to analyze the structure of the CNTs and defects present within the CNTs.

With the intention of the development of supercapacitor electrodes, VACNTs grown on aluminum foils were used in electrochemical measurements. Electrode samples were prepared from foils with sizes 2.5 cm × 1 cm, where a 0.5 cm^2 edge part of the foil was left empty for the attachment of contacts. To prevent CNT growth at the edge of the foils, polyimide tape was used to mask that particular area during catalyst deposition.

A three-electrode configuration was used for the electrochemical measurements of the supercapacitor electrodes. A potentiostat/galvanostat system (Gamry Reference 3000) was used for the measurements. The reference and counter electrodes were Ag/AgCl and platinum foil, respectively. All potentials were relative to the Ag/AgCl. Electrochemical behaviors of the electrodes were investigated by cyclic voltammetry, chronopotentiometry, potentiostatic electrochemical impedance spectroscopy in an aqueous 1 M sodium sulfate (Na_2SO_4) electrolyte solution.

3. Results and discussion

Photographs of aluminum foils following annealing and CNT growth are provided in Fig. 1(a). Slightly tinted yellow color for the foil on the left indicate the catalyst deposited areas, where upon growth turns into black.

TEM image of one of the CNTs is shown in Fig. 1(b). TEM analysis revealed that the obtained CNTs were multi-walled. Cross-sectional and top-view SEM images of the CNTs grown on

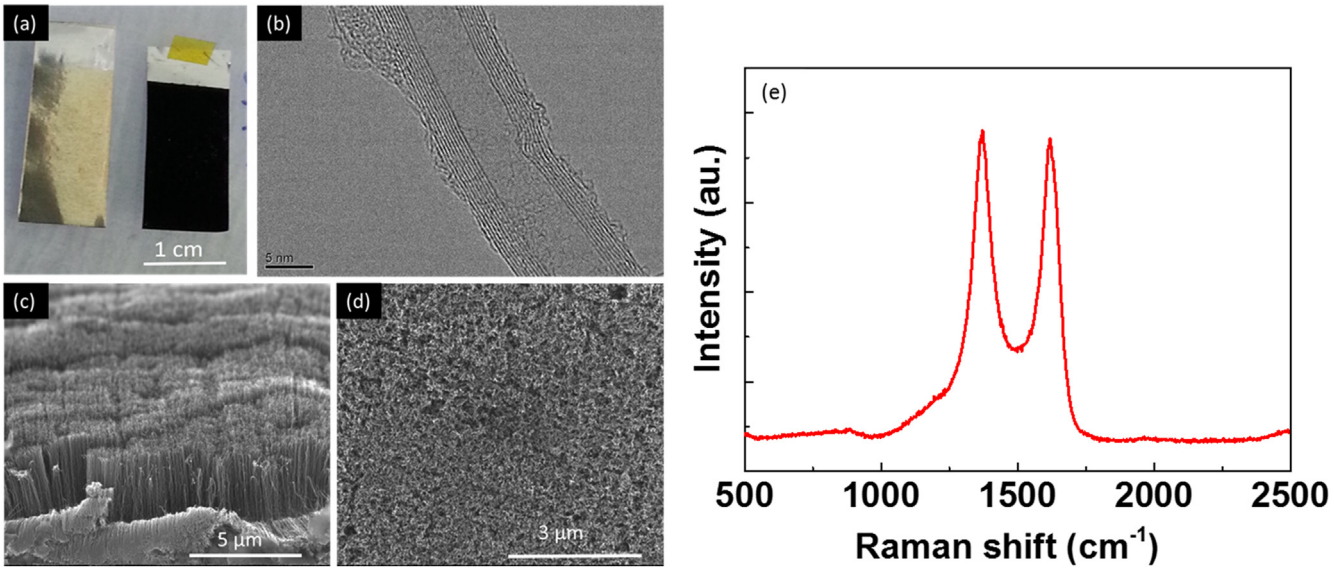

Fig. 1. (a) Photograph of the aluminum foils with catalyst (left) and grown CNTs (right). (b) TEM image, (c) cross-sectional and (d) top-view SEM images and (e) Raman spectrum of the CNTs grown on aluminum foils. (For interpretation of the references to color in this figure, the reader is referred to the web version of this article.)

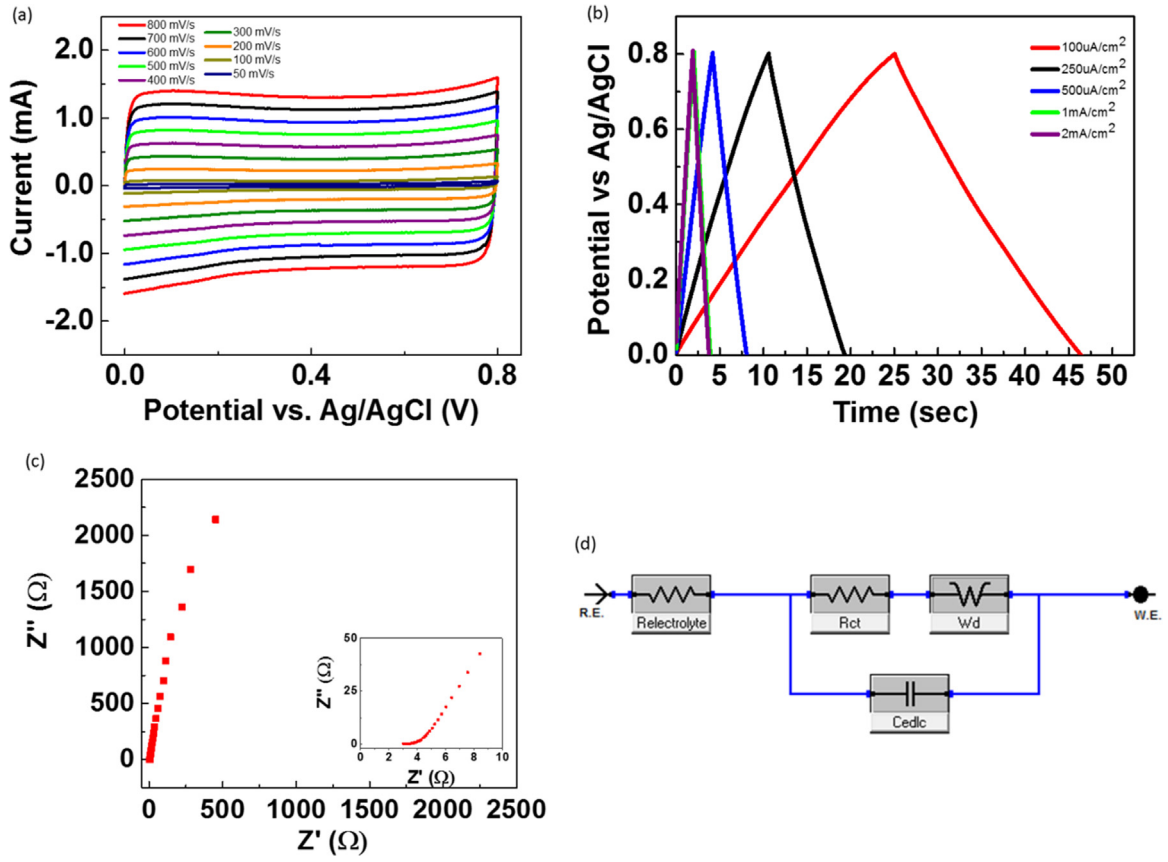

Fig. 2. (a) Cyclic voltammetry results of the VACNT electrodes at different scan rates, (b) galvanostatic charge-discharge characteristics of VACNT electrodes, (c) impedance spectra of the VACNT electrodes, (d) equivalent circuit used for the impedance analysis.

aluminum foils are provided in Fig. 1(c) and (d), respectively. VACNTs were found to be 4 μm long and quite uniformly grown on the aluminum foils. Raman spectrum of the CNTs grown on aluminum foils is provided in Fig. 1(e). The I_D/I_G ratio was found nearly 1 for this sample, indicating that the synthesized CNTs are defective and multiwalled, in agreement with TEM analysis.

For electrochemical measurements, aluminum foil was used as the current collector. Each VACNT acts as a parallel capacitive element contributing to the overall capacitance. Electrochemical measurements were performed within a potential window of 0 and 0.8 V. Fig. 2(a) shows the cyclic voltammetry (CV) results of the electrodes at different scan rates from 50 mV/s up to 800 mV/s. It is clear that the CV curves exhibit typical rectangular shapes at these scan rates, coinciding with the ideal electric double layer capacitor (EDLC) behavior [32].

Cyclic voltammetry results of the electrodes at different scan rates (5–800 mV/s) are provided in Fig. 2(a). Areal capacitance values of the electrodes at scan rates of 50, 100, 200, 300, 400, 500, 600, 700 and 800 mV/s were 0.71, 1.15, 1.8, 2.15, 2.33, 2.45, 2.52, 2.57 and 2.61 mF/cm^2, respectively. The galvanostatic charge-discharge (GCD) characteristics of the VACNT electrodes were measured at five different current densities of 100, 250, 500 μA/cm^2, 1 and 2 mA/cm^2 are provided in Fig. 2(b). GCD measurements were also conducted in between 0 and 0.8 V. The change in potential with time for both charging and discharging shows a symmetric and linear profile, even at current densities as high as 2 mA/cm^2, which is typical of EDLCs. It is also noticed that there is no major voltage drop upon the onset of discharging, showing that there is nearly no internal resistance. This is particularly important for the electrodes fabricated using CNTs. For CNT based electrodes, if CNTs are deposited onto a conducting substrate, series resistance always occurs resulting from the interface between the substrate and the CNTs [33]. However, in our case, since VACNTs are directly grown on aluminum foils, series resistance is almost negligible. This makes direct, one-step growth of VACNTs on metal foils an important route to fabricate supercapacitor electrodes. Further electrochemical behavior of the VACNT electrodes were investigated through impedance spectroscopy (EIS). The corresponding Nyquist plots within a frequency range of 50 kHz – 50 mHz is provided in Fig. 2(c). Equivalent circuit used for the impedance analysis is provided in Fig. 2(d), where $R_{electrolyte}$ is the resistance of interface between the electrode and electrolyte, R_{ct} is the charge transfer resistance, W_d is the Warburg component associated with diffusion of electrochemical species, and C_{edlc} is the capacitance of VACNTs.

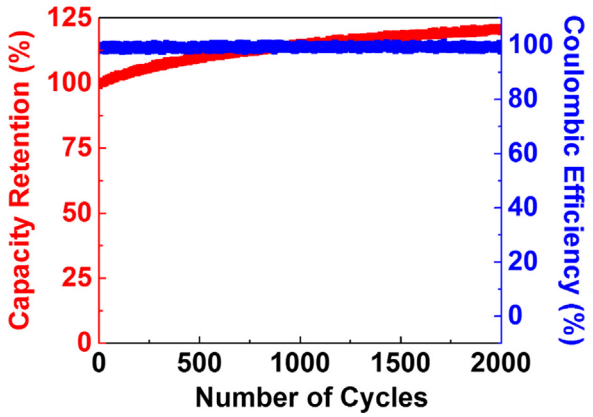

Fig. 3. Cycling performance in terms of the capacity retention and coulombic efficiency of VACNT electrodes measured through constant current charge-discharge at 0.1 mA/cm^2.

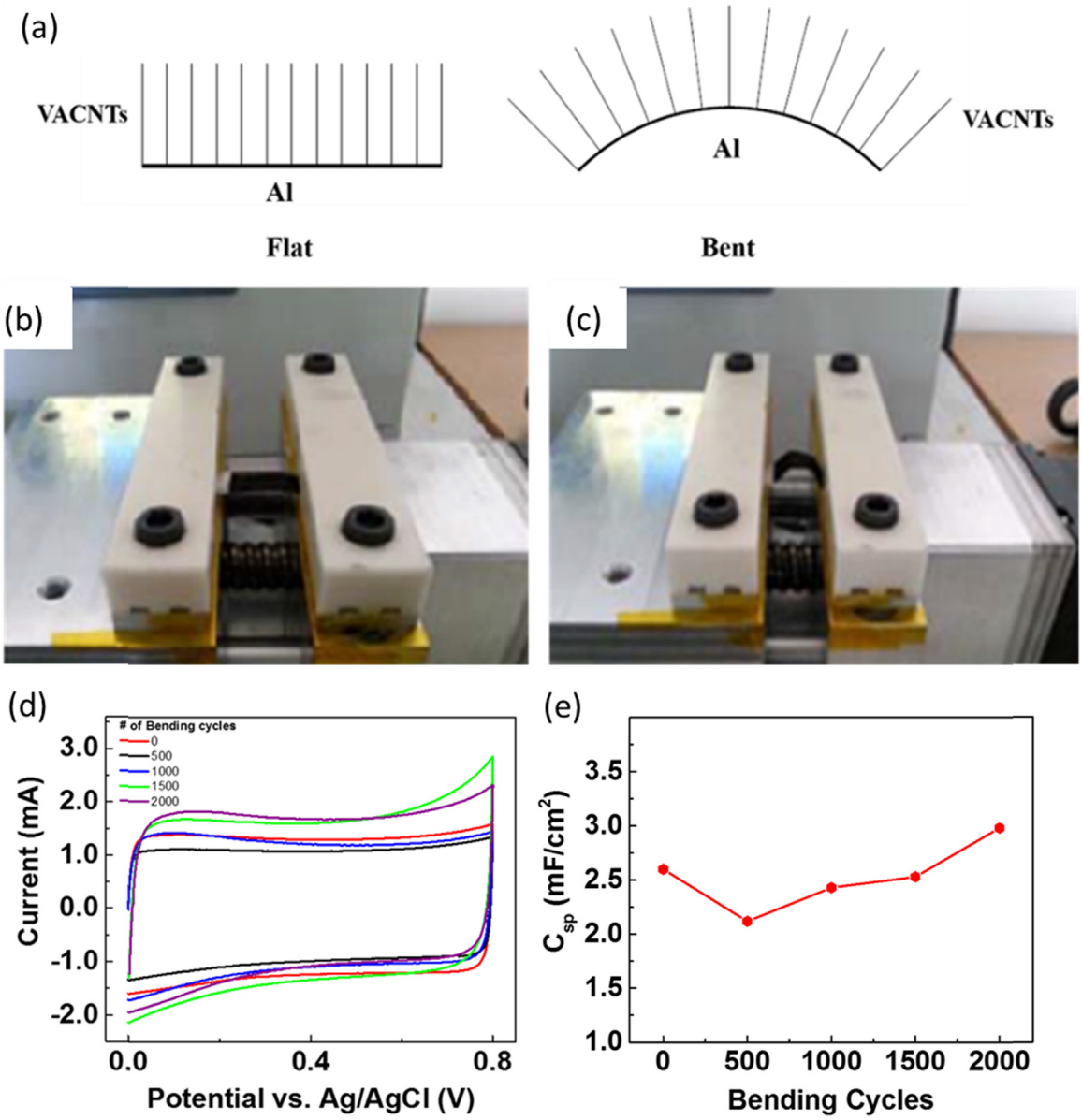

Fig. 4. (a) Schematics of VACNTs on aluminum foil when flat (left) and bent (right). Photographs of the bending setup with (b) flat and (c) bent VACNT electrodes. (d) CV and (e) areal capacitance results of the VACNT electrodes after each 500 bending cycles at a scan rate of 800 mV/s. Lines are for visual aid.

Supercapacitors behave as a resistance and capacitance in the high and low frequency regions, respectively. The nearly vertical line, parallel to imaginary axis, in Nyquist plot represents the ideal supercapacitor behavior and the absence of a semicircle in high frequency region indicates that there is negligible charge transfer resistance between the electrolyte and electrode. The intersecting point with real axis in the high frequency region points the equivalent resistance of the three electrode system, which is less than 3 Ω in this case. As discussed before, one-step and direct growth of VACNTs on aluminum foils initiates good contact between the CNTs and underlying aluminum foil and the electrodes formed with this method possess ideal supercapacitor characteristics. A typical equivalent circuit of the fabricated electrodes can be seen in Fig. 2(d). Although it gives an impression on how the charge storage affected by components such as the internal resistance or diffusion of ions, a real case is much more complicated. Complexity arises due to the fact that VACNTs create numerous parallel connected capacitive components on aluminum foil.

For further analysis, change in specific capacitance and coulombic efficiency for the VACNT supercapacitor electrodes during 2000 charge/discharge cycles are monitored. Electrode sample is charged and discharged at a current density of 0.1 mA/cm^2. Cyclic performance in terms of specific capacitance and coulombic efficiency of the VACNT electrode are provided in Fig. 3.

There is an improvement in the capacity retention of the electrodes for the investigated 2000 cycles. Cycling defines the submersion time of the electrodes into the electrolyte, which gradually improves the adsorption of electrolyte ions on hydrophobic VACNTs. Thus, the capacitance retention of the electrodes increased with cycling. Consequently, this is clearly showing the electrochemical as well as mechanical stability of the VACNTs on aluminum foils. Moreover, coulombic efficiencies are almost 100% for the investigated samples.

Growth of VACNTs on aluminum foils adds function to the foils, while still conserving their mechanical flexibility. Thus, it is possible to fabricate flexible supercapacitors using these electrodes. In order to evaluate the performance of flexible VACNT electrodes, a

custom build mechanical bending system is used. The sample is attached to the system from its short edges. The photographs of the foils with VACNTs in flat and flexed condition are provided in Fig. 4(a) and (b), respectively. Samples are loaded in tension and flexed down to a radius of curvature of 3.75 mm.

First, the CV measurement of the flat sample (denoted as 0 bending) is carried out. Then the foil is bent for 500 times and electrochemically tested again. This bending and measuring processes are repeated for 1000, 1500 and 2000 times. The CV graph of the sample at the end of each 500 bending cycles is provided in Fig. 4(c).

Similar CV characteristics are obtained for the samples, almost independent of the number of bending cycles. Measured areal capacitance values of the VACNT electrodes that are flat, 500, 1000, 1500 and 2000 times bent are 2.60, 2.12, 2.43, 2.53 and 2.98 mF/cm^2, respectively. It is clear that the performance of the VACNT electrodes get better upon bending although the capacitance drops after the first 500 cycles. It is highly possible that the initial drop in capacity occurs due to the disruption of initial morphology of VACNTs on foils. Following increase in the specific capacitance in further bending cycles; however, might be tentatively attributed to two reasons. First, bending cycles improve the mechanical adhesion between the VANCTs, which is electrostatic in origin upon CNT growth. Second, repetitive bending cycles enhance the penetration of electrolyte within the hydrophobic CNTs.

Bending operation with the set radius of curvature deformed the aluminum foil after 2000 cycles, thus the maximum number of bending cycles are designed as 2000 times. Therefore, it is the aluminum foil not the VACNTs that limit the flexibility of the electrodes. All in all, obtained results are quite promising, showing the potential of fabricated samples as flexible supercapacitor electrodes.

In this work, we preferred to report our results in areal capacitance instead of gravimetric capacitance. This is mainly because of the systematic errors that would occur during the measurement of electrode weight due to the low amount of active material.

4. Conclusions

VACNTs grown on aluminum foils are used as flexible supercapacitor electrodes. Aluminum is preferred as a cheap, flexible, conductive and readily available substrate for the CNT growth via CVD method. To deposit catalyst on aluminum foils, USP method is utilized as an easy method that can be performed in ambient conditions. We obtained a specific capacitance of 2.61 mF/cm^2 at a current density of 0.1 mA/cm^2. The electrodes preserved their electrochemical performance after 2000 bending cycles, which is found to be limited with the aluminum foil substrate not with the VACNTs. The methods and the materials used in this work are very simple, cost-effective and suitable for scale-up towards commercialization if desired. In that respect; however, detailed morphological characterization such as pore size distribution upon cycling and bending needs to be conducted.

Acknowledgements

This work was supported by the Scientific and Technological Research Council of Turkey (TUBITAK) under Grant no. 113E596.

References

[1] Fan Zhang, et al., Energy Environ. Sci. 6 (2013) 1623–1632.
[2] J. Gamby, et al., J. Power Sources 101 (2001) 109–116.
[3] Charan Masarapu, et al., ACS Nano 3 (2009) 2199–2206.
[4] Kristy Jost, et al., Energy Environ. Sci. 6 (2013) 2698–2705.
[5] Dale A.C. Brownson, E. Banks Craig, Chem. Commun. 48 (2012) 1425–1427.
[6] D. Kalpana, N.G. Renganathan, S. Pitchumani, J. Power Sources 157 (2006) 621–623.
[7] Li. Li Zhang, X.S. Zhao, Chem. Soc. Rev. 38 (2009) 2520–2531.
[8] Wen Lu, et al., J. Phys. Chem. Lett. 2 (2011) 655–660.
[9] A.H. Castro Neto, et al., Rev. Mod. Phys. 81 (2009) 109.
[10] H.B. Peng, et al., Appl. Phys. Lett. 83 (2003) 4238–4240.
[11] Shisheng Li, et al., Adv. Energy Mater. 1 (2011) 486–490.
[12] Gilbert D. Nessim, et al., Nano Lett. 9 (2009) 3398–3405.
[13] C. Zhang, et al., J. Appl. Phys. 108 (2010) 024311.
[14] M. Dharmendra, et al., Appl. Therm. Eng. 99 (2016) 61–71.
[15] Huan Pang, et al., J. Mater. Chem. A 1 (2013) 4177–4181.
[16] Kuniharu Takei, et al., Proc. Natl. Acad. Sci. 111 (2014) 1703–1707.
[17] Nishant Tripathi, et al., Appl. Nanosci. 5 (2015) 19–28.
[18] Dmitry G. Gromov, et al., Diam. Relat. Mater. 64 (2016) 97–102.
[19] Niels De Greef, et al., Diam. Relat. Mater. 51 (2015) 39–48.
[20] Meyya Meyyappan, et al., Plasma Sources Sci. Technol. 12 (2003) 205–216.
[21] Vincent Jourdain, Christophe Bichara, Carbon 58 (2013) 2–39.
[22] Bong Gill Choi, et al., ACS Nano 5 (2011) 7205–7213.
[23] Huhu Cheng, et al., Nanoscale 5 (2013) 3428–3434.
[24] Yanli Chen, et al., J. Power Sources 287 (2015) 68–74.
[25] Yingwen Cheng, et al., Nano Lett. 12 (2012) 4206–4211.
[26] Hao Zhang, et al., Nano Lett. 8 (2008) 2664–2668.
[27] Shisheng Li, et al., Adv. Energy Mater. 1 (2011) 486–490.
[28] Elizabeth A.H. Pilon-Smits, et al., Curr. Opin. plant Biol. 12 (2009) 267–274.
[29] Naoki Yoshikawa, et al., Nanotechnology 19 (2008) 245607.
[30] Susanne Dörfler, et al., J. Power Sources 227 (2013) 218–228.
[31] Aurelien Gohier, et al., Appl. Surf. Sci. 258 (2012) 6024–6028.
[32] Elzbieta Frackowiak, Francois Beguin, Carbon 39 (2001) 937–950.
[33] Qian Cheng, et al., Phys. Chem. Chem. Phys. 13 (2011) 17615–17624.